STScI | SPACE TELESCOPE SCIENCE INSTITUTE

Instrument Science Report ACS 2020-07

Unusual Horizontal Charge Overflow from Saturated CCD Pixels in the ACS WFC: Discovery and Remediation

Yotam Cohen
Melanie Kae Olaes
Norman A. Grogin

October 22, 2020

Abstract

When CCD pixels become saturated during an integration, excess charge may begin to spill over into neighboring pixels. This effect is commonly referred to as 'blooming', and the architecture of the CCD detector makes it such that this blooming is expected to occur only in the same column as the saturated pixel (vertically). However, for the ACS/WFC CCD, we recently noticed a previously-undocumented effect whereby a relatively small fraction ($\lesssim 10\%$) of excess charge from saturated pixels spills over into neighboring pixels in the same row (horizontally). In this report, we present the characteristics of this horizontal spilling of charge, or 'x-bloom', and a resulting pipeline to automatically identify and flag affected pixels. We demonstrate that proper accounting for the charge displaced by x-bloom, in addition to that lost to traditional vertical bloom, enables high accuracy photometry of arbitrarily saturated sources. This result can significantly increase the science value of archival WFC data, since a large fraction of archival images contain saturated sources which are subject to x-bloom.

1 Introduction

Saturation and blooming are related phenomena that occur in charge-coupled device (CCD) image sensors under conditions in which the finite charge capacity of a charge collection site of a pixel is exceeded. A pixel that has exceeded this capacity in a given exposure is said to be 'saturated', and the production of additional photo-electrons in such pixels results in an overflow, or 'blooming', of the excess electrons into adjacent device structures (Fellers & Davidson, 2006; Janesick, 2001). Some CCDs are designed and equipped with anti-blooming structures, which may provide a safe path for excess charge removal so that the blooming does not corrupt image data. The ACS/WFC CCD is not equipped with such technology, so saturation and blooming can cause a number of potentially undesirable effects in the detector output images. The most common and familiar of these effects are the bright streaks of pixels extending outward vertically (in detector coordinates) from saturated pixels, such as those near the center of bright stars (e.g. Figure 1). Typically, saturated pixels/sources are considered a nuisance and are regarded as unusable for several common science measurements. For example, standard PSF-fitting photometry/astrometry cannot be reliably performed on saturated stars since the streaks of bloomed pixels completely distort/corrupt the image of the source such that the PSF models no longer accurately capture the charge distribution of such sources.

For some users and research projects, however, saturated sources may actually be among the objects of interest in a given image. For this reason, it behooves us to understand whether saturated sources may be used for certain science calculations if handled appropriately. As an example, if there were some method by which accurate integrated photometry of saturated sources were possible, it could significantly increase the science value of archival and future image data containing saturated sources. Recently, Olaes et al. (2019) (hereafter Olaes+19) carried out a study of this topic, and found that most, but not all ($\lesssim 10\%$ discrepancy), of the expected light from saturated sources could be accounted for by including the light displaced by vertical blooming in the integrated photometry (Section 4). In any case, whether or not saturated sources are of interest to a given user, it is crucial that the affected pixels, and those corrupted by association, are flagged in the data quality arrays of ACS/WFC images during calibration, so that users and data processing routines (e.g. astrodrizzle) can handle them appropriately for their particular needs. The ACS calibration pipeline has always included some routines which flag saturated pixels, and Cohen & Grogin (2020) (hereafter CG20) have made significant improvements to these processing steps within the past year.

Recently however, we noticed that ACS/WFC images of saturated sources exhibit an additional, previously undocumented effect, in which a fraction of the excess charge from saturated pixels appears to bloom out horizontally (same row), in addition to the familiar and well-documented blooming in the vertical direction (same column). This effect is the subject of this report, and we hereafter refer to it as 'x-bloom' (as it occurs in the row-wise, or 'x', direction). The goals of this report are: 1) to document and present our findings about the x-bloom; 2) to demonstrate the machinery which we have developed to automatically identify affected pixels in ACS/WFC images; and 3) to show that accurate saturated source photometry can indeed be performed by accounting for pixels affected by x-bloom.

2 Characteristics of the x-bloom effect

In this section, we document some of the characteristics of the x-bloom effect, in order to prepare the reader to identify it in images, and to inform us about how we might develop some machinery to automatically identify it. First, we note that the x-bloom effect has only been observed in ACS/WFC images; it does not appear to occur in other HST cameras, past or present, e.g. ACS/HRC and WFC3/UVIS. Also, archival data reveal that the effect has been present throughout the entire history of the instrument, though it is not yet clear if/how its properties have changed over time.

Identification: An ACS/WFC image of a saturated star, exhibiting the typical way that the x-bloom effect manifests, is shown in Figure 1. The color-scale of this image is set using a logarithmic stretch and a min-max interval, which we find to be the best scale parameters for visual identification of the x-bloom – the effect can be easily missed, or mistaken for ordinary saturation or sky background, when using other combinations of scale parameters that do not differentiate it clearly. The saturated pixels in this image are lightly outlined in blue, and the x-bloom pixels in red. The automatic identification of the saturated pixels is done using the methodology described in CG20, while the automatic identification of the x-bloom pixels is done using the machinery that we develop and describe later in this work. Since CCD blooming is thought to only occur in the vertical direction (Janesick, 2001), we would expect the pixels in between the blue and red outlines in Figure 1 to be consistent with the local background, but they are actually significantly enhanced. This observation is the key to understanding how we can visually identify the x-bloom – it appears to the left and/or right of saturated pixels as a significant enhancement above the local background.

Extent: We see that the horizontal extent of the blooming appears to be roughly proportional to the width of the group of saturated pixels from which the x-bloom originates in a given pixel row. For example, near the very bottom of the vertical saturation trail of the star, where the number of saturated pixels in a given row is only one or two, the x-bloom also only extends out by one or two pixels. As we look up towards the center of the star though, where the number of saturated pixels in any given row of the saturation trail is greater, so too is the width of the x-bloom. This qualitative behavior is apparent in all examples that we inspected. The precise quantitative relationship however has proven difficult to establish due to large scatter, but it appears to be non-linear. We will expand on and make use of this empirical relationship when developing our x-bloom identification machinery later in this work.

Intensity: The intensity of the x-bloom appears to be correlated with the degree of over-saturation of the saturated pixels closest to it. For a given group of x-bloom pixels, the intensity tends to decrease with increasing horizontal distance away from the central group of saturated pixels, but it is not always monotonic. Typical intensities for the innermost x-bloom pixel are in the range of $\sim$ 16,000 to 22,000 e^- for those associated with highly saturated pixels, but they may be even higher in some cases, and may be arbitrarily low for those associated with minimally saturated pixels. For context, the typical saturation level of the WFC CCD is in the range of $\sim$ 75,000 to 85,000 e^-, meaning that the x-bloom pixels can be as bright as $\sim$ 25% of their saturated source pixel.

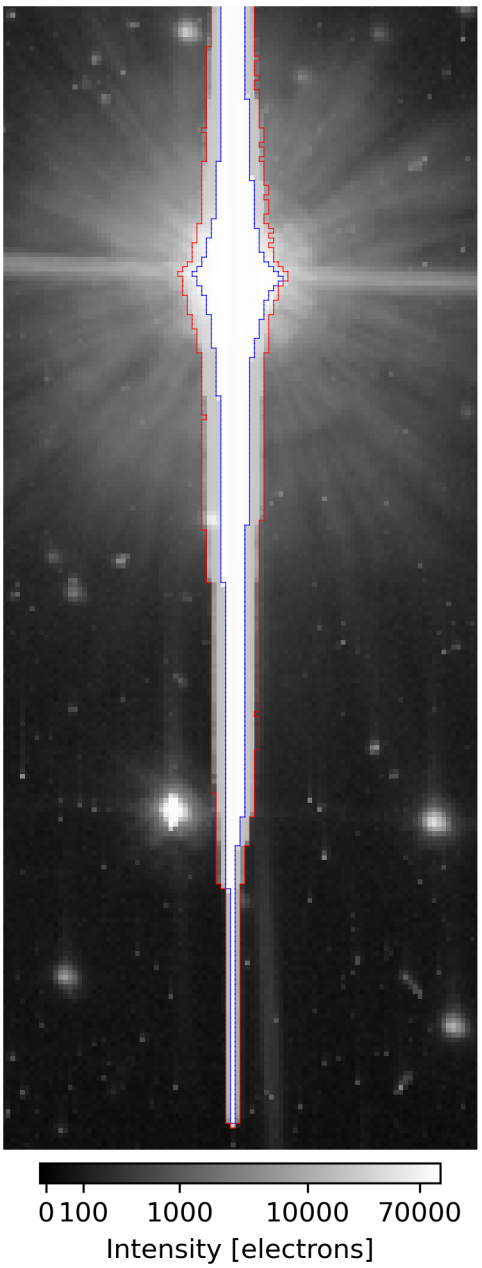

Figure 1: Cutout of a bright star from ACS/WFC image `jdg301bwq`, displayed using a logarithmic stretch and a min-max interval[1]. The pixels forming the core of the star are highly saturated, resulting in the traditional blooming effect, which manifests as the streaks of bright pixels extending vertically from the core of the star. In this work, we identify a newly documented effect in ACS/WFC images, dubbed x-bloom, which manifests as an additional blooming of excess charge from saturated pixels, but extending outward in the horizontal (x) direction, rather than vertical. These pixels affected by traditional bloom and x-bloom are lightly outlined in blue and red, respectively, in order to guide the eye. The ordinary bloomed pixels in this image have typical values of $\sim$ 80,000 to 90,000 e^-, whereas the x-bloomed pixels have typical values of $\sim$ 16,000 to 22,000 e^-.

[1]https://docs.astropy.org/en/stable/visualization/normalization.html

A question that naturally arose during our investigation of this effect is whether it is only associated with saturated pixels, or if x-bloom may occur for any given pixel, perhaps with an amplitude that depends on the intensity of the source pixel(s). Another relevant question is whether the x-bloom is actually a proper blooming effect that occurs on-chip during integration, like the familiar vertical blooming, or whether it occurs during readout, like the trails of charge left behind due to imperfect CCD charge transfer efficiency (CTE) (Ryon & Grogin, 2019, and references therein). Images of unsaturated stars do not appear to exhibit any significant enhancement above the expected brightness from PSF models, which suggests that the effect is not associated with unsaturated pixels. This is an important piece of information, but it is not entirely conclusive regarding the link between saturation and x-bloom, and it does not say anything about whether the effect occurs during integration or during readout. In order to explore these questions further and more conclusively, we turn to an analysis of so-called 'super-hot' pixels. These pixels are described in CG20, but, briefly, they are a set of hot pixels (Riess et al., 2002; Borncamp et al., 2017; McDonald et al., 2020) on the WFC CCD detector which typically have sufficiently high flux to saturate within a few tens of seconds of integration (i.e. dark current rates exceeding ~ 1000 e^-/s). Since these sources are generated within the detector, they are not convolved by the PSF, so their charge is, in principle, confined to a single pixel until they begin blooming. This feature of these sources allows us to use them as something of a 'controlled experiment' in which we can isolate the effects of blooming from other sources of charge.

As in CG20, for a given super-hot pixel, we collect a sample of image cutouts centered on the pixel from tens of thousands of archival ACS/WFC images, spanning orders of magnitude in integration time. We obtain the cutouts from fully-calibrated science images and background-subtract each cutout to account for variations in scene and sky level. We discard cutouts containing significant contribution from other sources (e.g. saturated bright stars). For a given super-hot pixel, we then make a series of plots like the ones shown in Figure 2. This figure focuses on one particular super-hot pixel and its immediately neighboring pixels on all four sides. Henceforth, we will refer to the neighboring pixels on the same side of the source pixel as the readout direction(s) as the downstream pixels, and the ones on the opposite side as the upstream pixels, consistent with previous relevant literature (e.g. Anderson & Bedin, 2010). For any given pixel, there are two upstream and two downstream neighbors, one of each for each readout direction. Plotted in the top panel of Figure 2 is the intensity of the super-hot pixel as a function of dark time, as well as a piecewise fit to the data, as described in CG20. Plotted in the middle and bottom panels are the same quantities but for the column-wise and row-wise neighbors, respectively, with the upstream and downstream pixels indicated by the different colored and shaped symbols. The three vertical dashed lines, and the corresponding encircled numbers, serve to delineate the three regimes of pixel integration as described in CG20. There are several important points to glean from this figure with respect to the aforementioned questions about the x-bloom:

- In the linear regime (labeled 1) of the integration of the source pixel, both the column- and row-wise upstream neighbors exhibit a clear non-zero intensity. This is expected and consistent with those upstream pixels being brightened by CTE losses during readout. Meanwhile, the brightness of the downstream pixels in both directions remains roughly constant in this regime, with a value consistent with the background residuals.

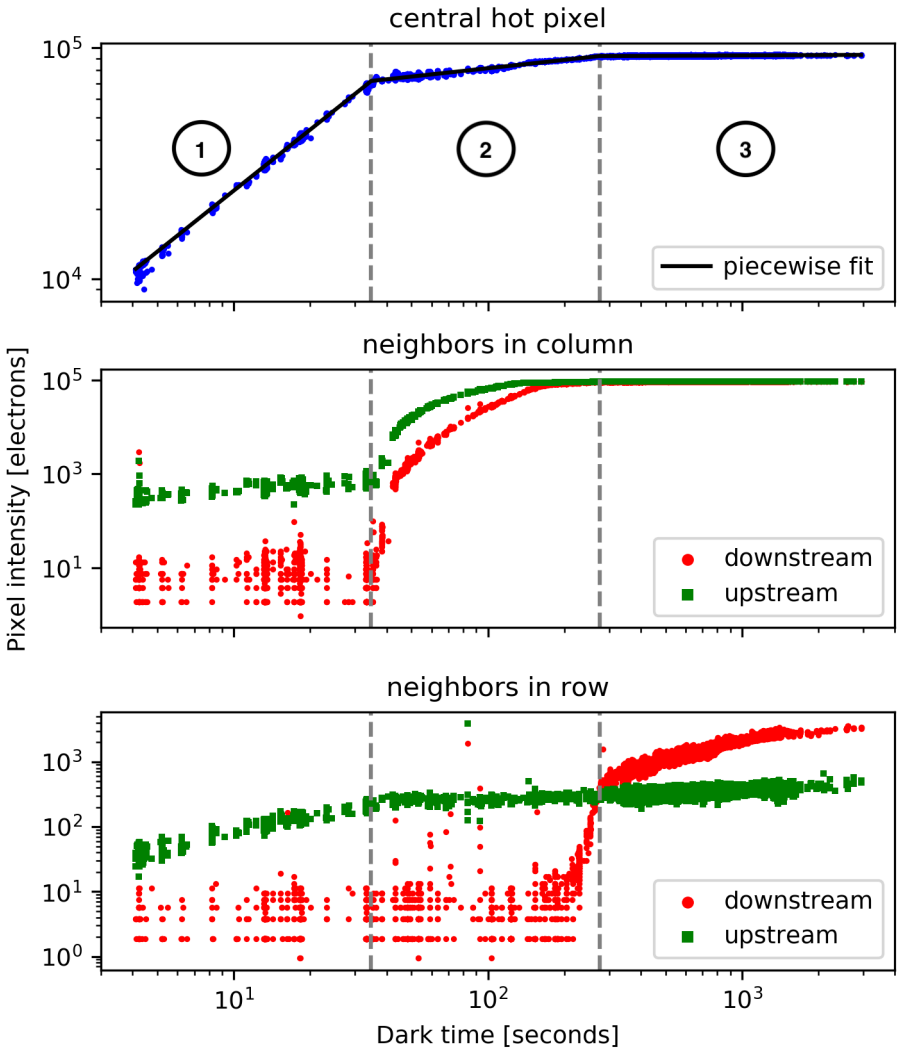

Figure 2: This figure shows the charge accumulation of a particular 'super-hot' pixel (top panel) on the ACS/WFC CCD detector, as well as its four immediately neighboring pixels (middle and bottom panels). As in Figure 2 of CG20, we plot the intensity as a function of dark (integration) time, measured using a large set of images spanning orders of magnitude in integration time. The super-hot pixel is saturated for integration times rightward of the first grey dashed line. The upstream/downstream convention used is such that CTE loss trails are expected to appear only in the upstream neighbors, while x-bloom may appear on either side, though in the case of this particular pixel, it is observed to appear only/primarily in the downstream neighbors, The key takeaways of this figure are that: 1) the row-wise downstream neighbor only begins to significantly brighten well into the saturated regime of the source pixel, indicating that x-bloom is associated with saturation, and 2) the row-wise downstream neighbor continues brightening with a large slope well into the regime where the source pixel intensity and CTE losses have nearly leveled out, indicating that the x-bloom occurs on-chip during integration, rather than during readout. Further information about the construction of the plot and about the super-hot pixels is given in the main text.

- At the start of the saturated regime (labeled 2) of the integration of the source pixel, both of the column-wise neighboring pixels begin to increase in intensity as charge blooms into them from the now-saturated source pixel. This manifests as the familiar vertical blooming effect. The row-wise upstream pixel intensity due to CTE losses

increases very gradually, commensurate with the marginal increase of the source pixel intensity in this regime. The row-wise downstream pixel remains consistent with the background until most of the way through this regime, during which time it suddenly begins to brighten, which appears as the x-bloom effect in the images. The behavior of the row-wise downstream pixel clearly suggests that the x-blooming effect is indeed associated only with saturated pixels, and that the onset may occur well into the saturated regime of the source pixel.

- In the final regime (labeled 3) of integration, the central super-hot pixel is fully saturated and asymptotically approaches its full-well value. In this regime, the row-wise upstream pixel is evidently still primarily or exclusively brightened by serial CTE losses, indicated by the very shallow slope of the brightening, commensurate with that of the super-hot pixel. On the other hand, the row-wise downstream neighbor is seen to brighten with a slope significantly steeper than the upstream neighbor. Under the hypothesis that x-bloom happens during readout, like CTE losses, we would expect the amplitude of the effect to only 'know' about the final value of the source pixel at readout, and thus asymptotically approach a certain value, similar to the behavior of the source pixel and the pixels brightened by CTE losses. However, what we actually see is that the intensity of the downstream pixel continues to increase significantly in this regime, much like the column-wise neighbors do in the middle regime. We believe that the most likely explanation for this is that the x-bloom actually happens during integration, like familiar vertical blooming, resulting in an amplitude that increases with increasing integration time irrespective of whether the source pixel has fully saturated or not. Put another way, the intensity of the x-bloom is correlated with the total amount of charge generated in the super-hot pixel during a given integration, rather than just the final charge level of super-hot pixel.

Upon inspection of this figure, the reader might question how the behavior of the row-wise neighbors of this super-hot pixel can be reconciled with the image in Figure 1. In particular, in Figure 1, the x-bloom appears on both the left and the right sides of the saturated pixels, whereas for the super-hot pixel in Figure 2, the effect is noticeable on only one side of the super-hot pixel. This observation highlights another curious property of the x-bloom effect – it does not always occur symmetrically, especially for smaller associations of saturated pixels like the super-hot pixels. In the sample of super-hot pixels that we analyzed, we find examples of all symmetry cases: some exhibit x-bloom predominantly on the upstream side, some predominantly on the downstream side, and some on both sides in roughly equal proportions. The particular super-hot pixel shown in Figure 2 was hand-picked as an example of one with little to no evidence of x-bloom on the upstream side, in order to isolate and distinguish between the effects of x-CTE losses and x-bloom.

On the other hand, for most of the images of strongly saturated stars that we visually inspected, the x-bloom does tend to be more symmetric. There are few, if any, cases of stars which have multiple pixels of x-bloom on one side, and none on the other, but there are many cases where the effect is slightly more extended on one side than the other, typically by not more than one or two pixels. The (a)symmetry of the x-bloom for a given saturated source appears to depend on the location on the CCD.

3 Machinery for Automatic Identification of x-bloom

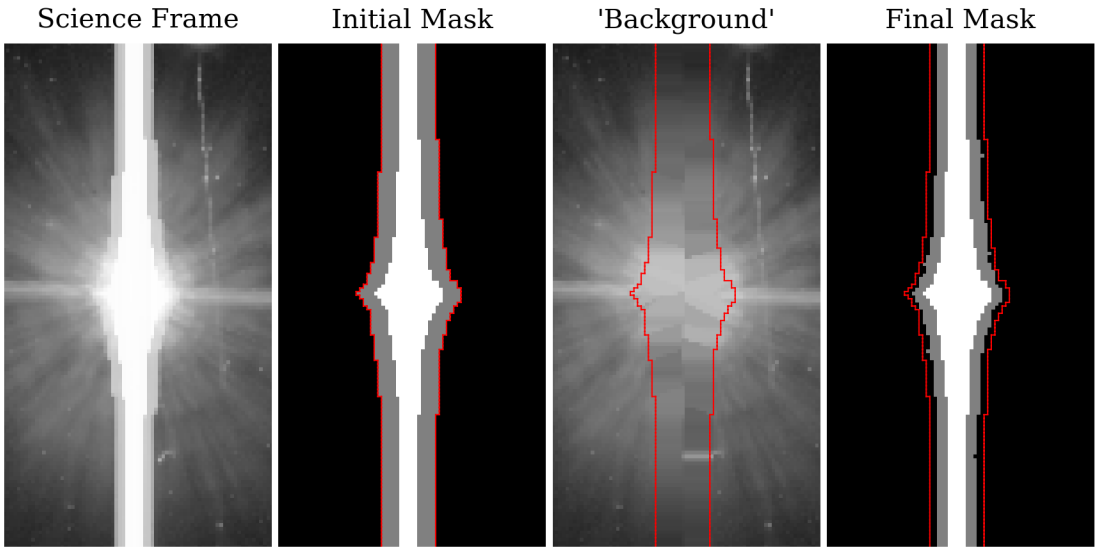

Figure 3: Using a cutout of a WFC image centered on a saturated star as an example, this figure shows some of the images and masks used/generated at the main steps of our x-bloom identification pipeline, in the order in which they are used. Full details of the processing steps are in the main text. From left to right:
Science Frame: Cutout of an ACS/WFC image centered on a highly saturated star. Both vertical blooming as well as x-bloom are visually apparent.
Initial Mask: The first mask generated by the pipeline. The mask has three different values: white for saturated pixels, grey for candidate x-bloom pixels, and black for neither. The boundary of the non-zero values of this mask is outlined in red and is superimposed onto the following panels. The saturated pixels are identified by checking the science frame against the WFC saturation level map, as described in CG20. The x-bloom pixel candidates are flagged by dilating the saturated pixel mask outward horizontally, with an extent that depends on the width of the group of saturated pixels a given row.
'Background': A modified version of the Science Frame in which all pixels contained in the Initial Mask have been removed and replaced with interpolated values from the surrounding pixels. The goal of this step is to approximate what the expected brightness would be in the x-bloom candidate pixels if there were no x-bloom, so that an elevation above this level in the original science frame can be detected.
Final Mask: Color scale is the same as the Initial Mask. The saturated pixel component of the mask is unchanged, but the x-bloom component has been refined by checking the values of the candidate x-bloom pixels in the science frame against the 'expected' values from the 'Background' image. Compared to the red outline of the Initial Mask, it can be seen that the refined mask has been pinched inwards by a few pixels. This refined mask more accurately captures the extent of the x-bloom pixels without overshooting. In other words, the Final Mask contains fewer x-bloom false positives compared to the Initial Mask.

Ideally, we would like to be able to correct ACS/WFC images for the x-bloom effect, restoring electrons to the pixels where they originated on the CCD. However, the stochastic and somewhat enigmatic way in which this effect manifests makes it considerably challenging to model accurately and self-consistently, so we will defer a full correction for future work. For the time being, it is important that we at least flag affected pixels so that users and data processing routines (e.g. astrodrizzle) may handle them appropriately for their particular needs. One of the main goals of our research on this topic was to develop such a tool which would automatically identify pixels affected by x-bloom. Our broad-brush concept for this

tool is relatively straightforward: Since the x-bloom appears to be exclusively associated with ordinary saturated pixels, the tool should create a mask of candidate x-bloom pixels by growing, or dilating, the mask of saturated pixels horizontally. This dilated mask could then be further refined to minimize false positives by performing some checks or calculations on each of the candidate pixels to identify those which actually exhibit a significant elevation above the expected brightness, and those that do not. We have developed such a tool, and we will now explain each of the steps in greater detail:

1. **Obtain the saturated pixel mask.** Since the x-bloom appears to originate and bloom outwards from ordinary saturated pixels, we can use a mask of saturated pixels as a starting point to look for the x-bloom. We obtain this mask by using the ACS/WFC saturation level map (CG20) to identify all the pixels in the science frame which are saturated.

2. **Identify all horizontal groups of saturated pixels and measure their widths.** When we refer to a 'horizontal group' of (saturated) pixels, we mean: one or more (saturated) pixels that are all immediately adjacent to each other in the same row of the image. For any given horizontal group of saturated pixels, the horizontal extent of the associated x-bloom appears to depend on the width of that saturated group. For this reason, we would like to treat pixel groups of different widths accordingly. We use `scipy.ndimage.label`, with a horizontal structuring element, to efficiently identify and label all horizontal groups of pixels in the saturated pixel mask, and we use the related `scipy.ndimage.labeled_comprehension` function to efficiently measure each of their widths.

3. **Dilate the saturated pixel mask(s).** Next, we use the `scipy.ndimage.binary_dilation` function to efficiently grow the saturated pixel mask(s) in the horizontal direction in order to create a mask containing the candidate x-bloom pixels. In order to handle each horizontal pixel group width accordingly, we first specify a mapping between the group width and the horizontal extent of the dilation on either side of the group. Then, for each (integer) pixel group width in a specified range, we create a temporary mask containing only pixel groups of the given width, and dilate that mask horizontally by the dilation width corresponding to that group width. We then combine all the temporary dilated masks into an initial 'master mask'. This mask has a certain value (e.g. 1) for saturated pixels, a different value (e.g. 2) for x-bloom candidate pixels, and a value of 0 everywhere else. If the specified mapping between saturated pixel group width and x-bloom width is highly accurate and globally consistent around the whole frame, then this initial master mask could in principle be used as the final master mask. However, further refinement can significantly improve the false positive rate.

4. **Refine the x-bloom mask.** We can refine the initial x-bloom mask by checking whether the candidate pixels are brighter than expected. There are several possible ways to go about this. For example, one could set a fixed intensity threshold informed by typical x-bloom levels in a given image. This approach runs the risk of a high false negative rate if the threshold is too high, and a high false positive rate if the threshold

is too low. We have found greater success using a different approach which is designed to check whether pixels are brighter than an estimate of their expected brightness in the absence of saturation and x-bloom. In this method, a temporary image of the local 'background' intensity is created by first masking out all the pixels in the initial master bloom mask (including both saturated pixels and x-bloom candidates), and then using the convolution methods in `astropy` to replace the values of the masked pixels with values interpolated from their neighbors. Ideally, far away from the cores of bright stars (i.e. far along the extended saturation trails of highly saturated stars), this 'background' image would be consistent with the sky level, while in the region surrounding the cores of bright stars, it would approximate the intensity of the extended stellar halo at a given radius from the core. The x-bloom candidate pixels in the original science frame are then checked against this check image, and only the pixels that are brighter than N times the corresponding pixels in the check image are flagged as x-bloom pixels in the final x-bloom mask. The factor N can be tweaked and specified by the user; we have found $N \approx 2$ to be a reasonable default value. With a careful choice of convolution kernel parameters and threshold factor N, and a suitable initial mask, this technique has proven to be powerful and effective for refining the x-bloom mask to better agree with our visual identification of the affected pixels. An example of such careful choices is to arrange that the initial dilation be quite generous and slightly overshoot the expected range of x-bloom so that the none of the x-bloom ends up in the convolution, since that would inflate the interpolated values.

There are a few important details of the above steps that we will now address. The mapping between the horizontal saturated pixel group width and the dilation width, used in Step 3, must be specified by the user. Our studies of the x-bloom have revealed that the relationship between the horizontal pixel group width and the corresponding x-bloom width is non-linear. There is also considerable scatter in the relationship due to the stochastic nature of the effect, but the overall form can be pieced together. In particular, we notice that the relationship is close to linear near a saturated pixel group width of zero, and quickly flattens out with increasing width. For pixel groups widths between 1 to ~ 5 pixels (often found along the extended vertical bloom trails of highly saturated stars, or the cores of modestly saturated stars), the width of the x-bloom on either side is almost always less than or equal to the width of the saturated group. On the other hand, for saturated pixel groups with widths between ~ 5 to ~ 20 pixels (for example, near the cores of highly saturated stars), the width of the x-bloom usually does not exceed ~ 5 to ~ 8 pixels. At the far extreme of this relationship, i.e. for groups of many tens of connected saturated pixels (for example, when observing extremely bright stars like Vega), the width of the x-bloom still almost never exceeds ~ 8 to ~ 11 pixels. We have also noticed that this relationship differs slightly between the two CCDs of the WFC detector, in the sense that WFC2 tends to have wider x-bloom for a given saturated pixel group width. We have provided a default mapping in the tool which seems to provide good fiducial results for majority of cases. However, we strongly recommend users of this tool to visually inspect the initial masks and the science frames side-by-side, and tweak the mapping accordingly for the images they are working on.

Another detail worth discussing is the specifics of the convolution methods used to produce the 'background' image. If using a single convolution kernel for the whole frame (most

likely scenario), the kernel must be at least as wide as the widest horizontal group of pixels in the initial mask, otherwise proper interpolation is not possible, but too large will result in a loss of fidelity. By default, we have specified a gaussian kernel with a width determined by the widest pixel group in the mask plus one, but we recommend that users tweak these parameters, in concert with the initial mask dilation mapping, until satisfactory results are achieved for the particular images they are working on.

At the time of this writing, the main components of this tool, as well as a worked example, are available for inspection in the following publicly-available jupyter notebook: `https://www.stsci.edu/~ycohen/work/xbloom/`. In the future, we plan to integrate this code into a proper python module, and/or integrate it into the ACS calibration pipeline.

4 Results: Improved Photometry on Saturated Sources

The vertical bloom trails extending from saturated sources make it difficult or impossible to perform typical aperture or PSF-fitting photometry on them; most authors completely ignore these sources for their analyses. In Olaes+19, an innovative method for performing photometry on saturated sources was developed and explored, with considerable success. These authors used a custom mask for each saturated source, consisting of a standard circular aperture component, as well as an extended component constructed from the saturated pixel mask of the data quality arrays, in order to account for the charge in the vertical bloom trails (see their Figure 3). As shown in their Figures 6 and 7, the brightness integrated within these custom masks is much closer to the expected value as compared to that measured using just a simple circular aperture. However, there still exists a discrepancy for saturated sources that increases with increasing source brightness, with as much as $\sim 10\%$ of the expected charge still unaccounted for at the extreme bright end of their sample.

One of the goals of our research on the x-bloom was to understand whether the charge displaced horizontally due to this effect can account for the remaining missing charge in the analysis of Olaes+19. To that end, we reproduced the photometry shown in their Figure 7, but also performed an additional run of the photometry using our full mask which includes both saturated pixels as well as x-bloom pixels. We also folded in one additional image pair (jdg302clq_flc.fits and jdg301bwq_flc.fits) from the same set of visits in order to increase the sample size. For each image pair, a sample of stars that are unsaturated in the 'short' exposure, but saturated in the 'long' exposure, were photometered using the three different methods for the 'long' exposure, and using a standard circular aperture in the 'short' exposure. The results are shown in our Figure 4, which has effectively the same axes as Figure 7 of Olaes+19. The horizontal axis shows the 'short' exposure brightness, and the vertical axis shows the ratio of the brightness in the 'long' exposure to the 'short' exposure, scaled by the ratio of their exposure times. The resulting quantity on the vertical axis is effectively the ratio of measured to expected brightness, assuming that we should expect the brightness in the 'long' exposures to be equal to the brightness in the 'short' exposures, scaled up by the exposure time. The three different sets of marker colors/symbols represent the three different masks used to perform the photometry of the saturated sources in the 'long' exposure images. Just like in Figure 7 of Olaes+19, the orange symbols are the circular aperture photometry, and the blue symbols are the photometry using a custom mask consisting of the

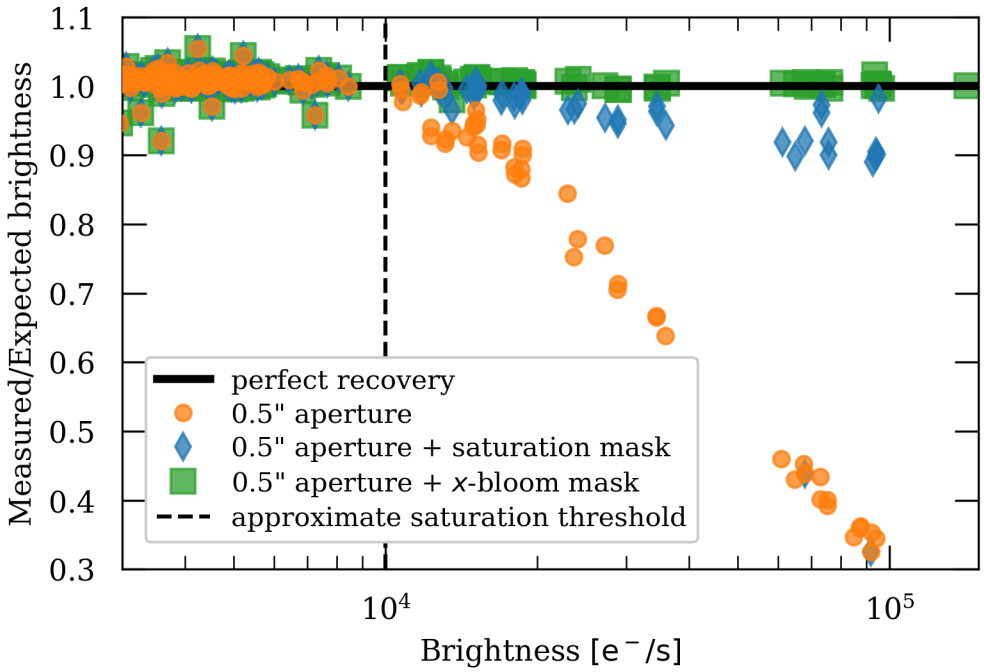

Figure 4: This figure is similar to Figure 7 of Olaes+19. It shows the results of performing photometry on stars in ACS/WFC images of star cluster 47 Tuc. The photometry was performed on pairs of images, with each pair consisting of one 'short' and one 'long' exposure of the same pointing. Plotted on the horizontal axis is the aperture photometry from the 'short' exposures, in which all the stars are unsaturated. Plotted on the vertical axis is the ratio of the 'long' exposure photometry to the 'short' exposure photometry, scaled by the ratio of the exposure times. The different symbols correspond to the three different methods used to photometer the 'long' exposures, as indicated in the legend and described in detail in the main text. The grey, dashed, vertical line indicates the approximate brightness at which saturation begins. The key takeaways of this figure are as follows: Using simple aperture photometry (orange circles) on saturated sources results in large errors, as expected since much of the charge is in vertical bloom trails. Accounting for the vertical bloom trails (blue diamonds) significantly improves the result, but there is still a discrepancy in the measured/expected brightness. However, accounting for both the vertical bloom trails *and* the x-bloom (green squares) results in essentially perfect recovery of all the expected charge, even for extremely saturated sources.

circular aperture as well as saturated pixels. The green symbols are the photometry using our updated custom mask, consisting of the same circular aperture and saturated pixel mask as for the blue symbols, but also including a component accounting for the x-bloom pixels. This additional x-bloom component is the direct output of our x-bloom detection machinery described above, which we ran on these images.

The primary result is that, by accounting the charge lost to x-bloom, in addition to the circular aperture and saturated pixels, the expected charge is essentially perfectly recovered, and without any notable excess. This result is impactful to researchers because a large fraction of ACS/WFC images contain saturated sources, which are usually ignored/discarded, but can now be reliably photometered and added to source catalogs. These saturated sources are still unsuitable for precise astrometry or PSF-modeling – among other types of measurements – but for analyses involving just the integrated brightness of a source, e.g. color-magnitude diagrams and stellar luminosity functions, this machinery provides a way for

saturated sources to be included. Separately, this machinery also allows all the charge from saturated sources to be masked out of images more accurately, which can help in generating more accurate background maps.

5 Conclusions, Recommendations, and Future Work

In this work, we reported on the discovery and characteristics of an unexpected effect that occurs in the ACS/WFC CCD, in which some charge from saturated pixels overflows into neighboring pixels in the horizontal direction – we dub this effect 'x-bloom'. The exact cause of this effect is currently unknown, but it appears to have been present throughout the entire lifetime of ACS/WFC, and such an effect does not appear to occur for any other HST cameras, past or present. The magnitude of the charge displaced due to this effect can amount to a significant fraction ($\lesssim 10\%$) of the total charge associated with a given saturated source.

By using empirically-derived properties of the x-bloom, we developed some prototype machinery that attempts to automatically identify affected pixels in WFC images. This machinery appears to be successful, as confirmed by visual inspection, and by photometry. The ACS team is currently considering if/how to incorporate this machinery into calibrated WFC data products. In the meantime, ACS users whose science data/calculations may be adversely affected by x-bloom are encouraged to contact the ACS help desk for personalized guidance.

There are still several open questions about this effect and its consequences. For example: How does x-bloom affect background estimation in images with significant coverage by saturated pixels? Is it possible to predict or model the detailed behavior of the x-bloom, allowing for it to be corrected for, rather than just flagged? Does x-bloom result in any undesirable effects in combined science frames (e.g. using astrodrizzle), and, if so, is it possible to mitigate them by flagging the affected pixels and handling them properly during image combination? We plan to explore these topics in future work, and we encourage any readers who may have further insight or information to contact the ACS team.

Acknowledgements

We thank the ACS team for their helpful discussions, review, and support of this work. This work made use of: NumPy (Van Der Walt et al., 2011), SciPy (Virtanen et al., 2019), matplotlib (Hunter, 2007), and Astropy (Price-Whelan et al., 2018).

References

Anderson, J., & Bedin, L. 2010, An Empirical Pixel-Based Correction for Imperfect CTE. I. HST's Advanced Camera for Surveys, Tech. rep.

Borncamp, D., Grogin, N., Bourque, M., & Ogaz, S. 2017, Pixel History for Advanced Camera for Surveys Wide Field Channel, Tech. rep.

Cohen, Y., & Grogin, N. A. 2020, New and Improved Saturated Pixel Flagging for the ACS/WFC, Instrument Science Report ACS 2020-2

Fellers, T. J., & Davidson, M. W. 2006, Concepts in Digital Imaging Technology

Hunter, J. D. 2007, Computing In Science & Engineering, 9, 90

Janesick, J. R. 2001, Scientific charge-coupled devices

McDonald, M. C., Desjardins, T. D., & Miles, N. D. 2020, Anneal Efficacy in the Advanced Camera for Surveys Wide Field Channel, Instrument Science Report ACS 2020-5

Olaes, M., Hoffmann, S., & Bellini, A. 2019, Assessing the Accuracy of Relative Photometry on Saturated Sources with ACS/WFC, Instrument Science Report ACS 2019-3

Price-Whelan, A. M., Sipőcz, B. M., Günther, H. M., et al. 2018, Astronomical Journal, 156, 123

Riess, A., Mutchler, M., & van Orsow, D. 2002, A First Look at Hot Pixels on ACS, Tech. rep.

Ryon, J. E., & Grogin, N. A. 2019, ACS/WFC Parallel CTE from EPER Tests, Tech. rep.

Van Der Walt, S., Colbert, S. C., & Varoquaux, G. 2011, Computing in Science & Engineering, 13, 22

Virtanen, P., Gommers, R., Oliphant, T. E., et al. 2019, arXiv e-prints, arXiv:1907.10121